MR Spectroscopy of the Cervical Spinal Cord in Chronic Spinal Cord Injury

Wyss, Patrik O ; Huber, Eveline ; Curt, Armin ; Kollias, Spyros ; Freund, Patrick ; Henning, Anke

Abstract: Purpose To investigate metabolic changes in chronic spinal cord injury (SCI) by applying MR spectroscopy in the cervical spinal cord. Materials and Methods Single-voxel short-echo spectroscopic data in study participants with chronic SCI and healthy control subjects were prospectively acquired in the cervical spinal cord at C2 above the level of injury between March 2016 and January 2017 and were compared between groups. Concentrations of total N-acetylaspartate (tNAA), myo-inositol (mI), total choline-containing compounds (tCho), creatine, and glutamine and glutamate complex were estimated from the acquired spectra. Participants were assessed with a comprehensive clinical evaluation investigating sensory and motor deficits. Correlation analysis was applied to investigate relationships between observed metabolic differences, lesion severity, and clinical outcome. Results There were 18 male study participants with chronic SCI (median age, 51 years; range, 30-68 years) and 11 male healthy control subjects (median age, 45 years; range, 30-67 years). At cervical level C2, tNAA/mI and tCho/mI ratios were lower in participants with SCI (tNAA/mI: -26%, P = .003; tCho/mI: -18%; P = .04) than in healthy control subjects. The magnitude of difference was greater with the severity of cord atrophy (tNAA/mI: R = 0.44, P = .003; tCho/mI: R = 0.166, P = .09). Smaller tissue bridges at the lesion site correlated with lower ratios of tNAA/mI (R = 0.69, P = .006) and tCho/mI (R = 0.51, P = .03) at the C2 level. Lower tNAA/mI and tCho/mI ratios were associated with worse sensory and motor outcomes (P < .05). Conclusion Supralesional metabolic alterations are observed in chronic spinal cord injury, likely reflecting neurodegeneration, demyelination, and astrocytic gliosis in the injured cervical cord. Lesion severity and greater clinical impairment are both linked to the biochemical changes in the atrophied cervical cord after spinal cord injury. © RSNA, 2019 Online supplemental material is available for this article. See also the editorial by Lin in this issue.

DOI: https://doi.org/10.1148/radiol.2018181037

Radiology

ORIGINAL RESEARCH • NEURORADIOLOGY

MR Spectroscopy of the Cervical Spinal Cord in Chronic Spinal Cord Injury

Patrik O. Wyss, MSc • Eveline Huber, MSc* • Armin Curt, MD • Spyros Kollias, MD • Patrick Freund, MD, PhD • Anke Henning, PhD*

From the Institute for Biomedical Engineering, University and ETH Zurich, Gloriastrasse 35, CH-8092 Zurich, Switzerland (P.O.W., A.H.); Department of Radiology, Swiss Paraplegic Centre, Nottwil, Switzerland (P.O.W.); Max Planck Institute for Biological Cybernetics, Tuebingen, Germany (P.O.W., A.H.); Spinal Cord Injury Center, University Hospital Balgrist, University of Zurich, Zurich, Switzerland (E.H., A.C., P.F.); Institute of Neuroradiology, University Hospital, Zurich, Switzerland (S.K.); Department of Brain Repair and Rehabilitation, UCL Institute of Neurology, University College London, England (P.F.); Wellcome Trust Centre for Neuroimaging, UCL Institute of Neurology, University College London, England (P.F.); Department of Neurophysics, Max Planck Institute for Human Cognitive and Brain Sciences, Leipzig, Germany (P.F.); and Institute of Physics, Ernst-Moritz-Arndt University Greifswald, Greifswald, Germany (A.H.). Received May 1, 2018; revision requested June 6; final revision received October 24; accepted December 3. **Address correspondence to** P.O.W. (e-mail: *pawyss@biomed.ee.ethz.ch*).

Study funded by Schweizerischer Nationalfonds zur Förderung der Wissenschaftlichen Forschung (143715), Hartmann Müller-Stiftung für Medizinische Forschung (2047), Universität Zürich (Clinical Research Priority Program Multiple Sclerosis), H2020 European Research Council (SYNAPLAST MR, grant no. 679927), and Wings for Life (WFL-CH-007/14).

*P.O.W. and E.H. contributed equally to this work.

Conflicts of interest are listed at the end of this article.

See also the editorial by Lin in this issue.

Radiology 2019; 291:131–138 • https://doi.org/10.1148/radiol.2018181037 • Content codes: BQ MR NR

Purpose: To investigate metabolic changes in chronic spinal cord injury (SCI) by applying MR spectroscopy in the cervical spinal cord.

Materials and Methods: Single-voxel short-echo spectroscopic data in study participants with chronic SCI and healthy control subjects were prospectively acquired in the cervical spinal cord at C2 above the level of injury between March 2016 and January 2017 and were compared between groups. Concentrations of total *N*-acetylaspartate (tNAA), myo-inositol (mI), total choline-containing compounds (tCho), creatine, and glutamine and glutamate complex were estimated from the acquired spectra. Participants were assessed with a comprehensive clinical evaluation investigating sensory and motor deficits. Correlation analysis was applied to investigate relationships between observed metabolic differences, lesion severity, and clinical outcome.

Results: There were 18 male study participants with chronic SCI (median age, 51 years; range, 30–68 years) and 11 male healthy control subjects (median age, 45 years; range, 30–67 years). At cervical level C2, tNAA/mI and tCho/mI ratios were lower in participants with SCI (tNAA/mI: −26%, $P = .003$; tCho/mI: −18%; $P = .04$) than in healthy control subjects. The magnitude of difference was greater with the severity of cord atrophy (tNAA/mI: $R^2 = 0.44$, $P = .003$; tCho/mI: $R^2 = 0.166$, $P = .09$). Smaller tissue bridges at the lesion site correlated with lower ratios of tNAA/mI ($R^2 = 0.69$, $P = .006$) and tCho/mI ($R^2 = 0.51$, $P = .03$) at the C2 level. Lower tNAA/mI and tCho/mI ratios were associated with worse sensory and motor outcomes ($P < .05$).

Conclusion: Supralesional metabolic alterations are observed in chronic spinal cord injury, likely reflecting neurodegeneration, demyelination, and astrocytic gliosis in the injured cervical cord. Lesion severity and greater clinical impairment are both linked to the biochemical changes in the atrophied cervical cord after spinal cord injury.

Online supplemental material is available for this article.

Spinal cord injury (SCI) results in permanent sensorimotor deficits and remote neurodegeneration and reorganization along the neuroaxis, all of which have strong relationships with clinical outcomes (1,2). These relationships are of high clinical relevance because in vivo neuroimaging assessing volumetric and microstructural changes of the central nervous system might help to improve prediction of outcome and stratification of patients in future interventional trials (3).

To understand biochemical alterations in the atrophied cervical cord (1) after chronic SCI, proton MR spectroscopy is the tool of choice because it allows noninvasive characterization of metabolic alterations. The spinal cord is one of the most difficult areas within the central nervous system to interrogate by using MR spectroscopy because of the low signal-to-noise ratio and magnetic field homogeneity owing to its deep location and the heterogeneity of the surrounding tissue. The quality of spinal cord MR spectroscopy has recently improved (4), and this modality has been applied to the spinal cords of patients with different neurologic diseases, including multiple sclerosis (5), amyotrophic lateral sclerosis (6), and Friedreich ataxia (7). Preliminary results in patients with chronic SCI from a different cohort have been published previously (8–10). However, to our knowledge, metabolic changes in chronic SCI have not yet been systematically investigated.

In this study, we investigated metabolic alterations in the atrophied spinal cord above the level of injury at vertebral level C2. We assessed the relationship of these alterations to spinal cord atrophy, lesion severity, lesion level, the completeness of injury, and clinical impairment using short-echo proton MR spectroscopy.

Preclinical literature shows demyelination and altered cell and membrane integrity along with activated

Abbreviations

Cr = creatine, Glx = glutamine and glutamate complex, mI = myo-inositol, SCA = spinal cord area, SCI = spinal cord injury, SCIM = Spinal Cord Independence Measure, tCho = total choline-containing compounds, tNAA = total *N*-acetylaspartate

Summary

In patients with chronic spinal cord injury, metabolic alterations are detected superior to the spinal cord lesion level at MR spectroscopy. These alterations likely reflect neurodegeneration, demyelination, and astrocytic gliosis in the injured cervical cord.

Implications for Patient Care

- MR spectroscopy shows biochemical changes above the level of spinal cord injury.
- Lower total *N*-acetylaspartate-to-myo-inositol and choline-containing compounds-to-myo-inositol ratios at MR spectroscopy were associated with worse sensory and motor outcomes ($P < .05$).

astrocytes (11) remote to the site of traumatic SCI. Patients with chronic SCI are thus expected to exhibit altered metabolism in the atrophied cervical cord above the level of injury. Owing to cell and membrane integrity alteration and demyelination, total choline-containing compounds (tCho), creatine (Cr), and total *N*-acetylaspartate (tNAA) may be lower in chronic SCI, whereas astrocytic gliosis would result in higher concentrations of myo-inositol (mI). We therefore investigated three ratios, tNAA/mI, tCho/mI, and Cr/mI, with the hypothesis that each metabolite would be lower in patients with chronic SCI than in healthy control subjects.

Materials and Methods

The local ethics committee of Zurich approved our study (KEK-ZH-No.2014-610, PB2016-00126), which was conducted in accordance with the Declaration of Helsinki. All participants were informed about the aim and procedure of this prospective study prior to measurement and gave written informed consent.

Participants

We recruited participants for this study between March 2016 and January 2017. Inclusion criteria for participants with SCI were as follows: *(a)* chronic traumatic injury (>1 year after injury), *(b)* no other neurologic or mental disorders, and *(c)* ability to undergo MRI. All participants had no preexisting neurologic, mental, or medical disorders affecting functional outcome. One patient had to be excluded because he did not fit into the neurovascular coil.

Experimental Design

Clinical assessments.—Participants with SCI underwent a clinical evaluation (E.H., with 5 years of experience) that included *(a)* the International Standards for Neurological Classification of Spinal Cord Injury protocol (12) for motor, light touch, and pinprick scores and *(b)* the Spinal Cord Independence Measure (SCIM) to measure daily life independence (13). All participants completed the full protocol.

MRI protocol.—The study was performed with a 3.0-T Philips MRI unit (Achieva, release 3.2.3; Philips Healthcare, Best, the Netherlands) by using a 16-channel sensitivity-encoding neurovascular coil (Philips Healthcare) to acquire spectra from the cervical cord above the level of injury (Fig 1). MRI measurement sequences included a survey acquisition, anatomic acquisitions, and spectroscopic measurements (total examination duration: 45 minutes).

At the C2 level, we used a T2-weighted image (repetition time msec/echo time msec, 3000/120; flip angle, 90°; in-plane resolution, 0.5 × 0.5 mm; section thickness, 3.2 mm) to place the spectroscopic volume of interest (dimensions: 6 mm × 9 mm × 35 mm, 1.9 mL). We applied the metabolite cycling point-resolved spatially localized spectroscopy, or PRESS, technique (2000–2500 [heartbeat triggered]/30; number of signals acquired, 512; spectral bandwidth, 2000 Hz; readout duration, 512 msec; imaging time, 35 minutes), as described previously (4). It included higher-order shimming, broadband outer volume suppression, and inner volume saturation to minimize the chemical shift displacement, resulting in a smaller effective voxel size (5.5 mm × 7.5 mm × 31 mm, 1.3 mL) (shown as a red box in Fig 1). We split the spectroscopic acquisition in measurement acquisition blocks of 128 or 256 signal averages and readjusted the volume of interest on the basis of an updated T2 image to minimize participant motion.

At the lesion site, we performed anatomic MRI sequences for all tetraplegic (ie, quadriplegic) participants. Each of these participants had previously undergone an MRI examination performed with a 1.5-T (two participants) or 3.0-T (seven participants) Siemens MRI unit (Siemens Healthcare, Erlangen, Germany). At the center of the lesion, a sagittal T2-weighted image (for 1.5 T: 4125/106 and flip angle, 150°; for 3.0 T: 3500/84 and flip angle, 160°) was acquired to assess lesion severity.

MRI Postprocessing

Postprocessing and quantification of spectroscopic data.—We reconstructed spectroscopic data using the commercially available MRecon framework (version 3.0.530; GyroTools, Zurich, Switzerland) in MATLAB 2014b (version 8.3.0.532; MathWorks, Natick, Mass). We used non–water-suppressed frequency-aligned measurement series (4) with truncation and zero filling in the time domain after 200 msec before quantification by LCModel (6.3–1M) (14). Metabolic concentration values are expressed as ratios to mI or Cr, because absolute quantification through internal water referencing in the spinal cord is not reliable because of the pulsating surrounding cerebrospinal fluid (see Fig E1 [online]). The basis set for spectral reconstruction included the following metabolites: *N*-acetylaspartate (NAA), *N*-acetylaspartylglutamate (NAAG), glutamate (Glu), glutamine (Gln), glycerophosphocholine (GPC), phosphocholine (PCh), Cr, scyllo-inositol (sI), and mI. Because of strongly overlapping resonance lines, we combined the spectra of the following metabolites: NAA plus NAAG equals tNAA, GPC plus PCh equals tCho, and Gln plus Glu complex equals Glx. Following the recommendation of the consensus discussion

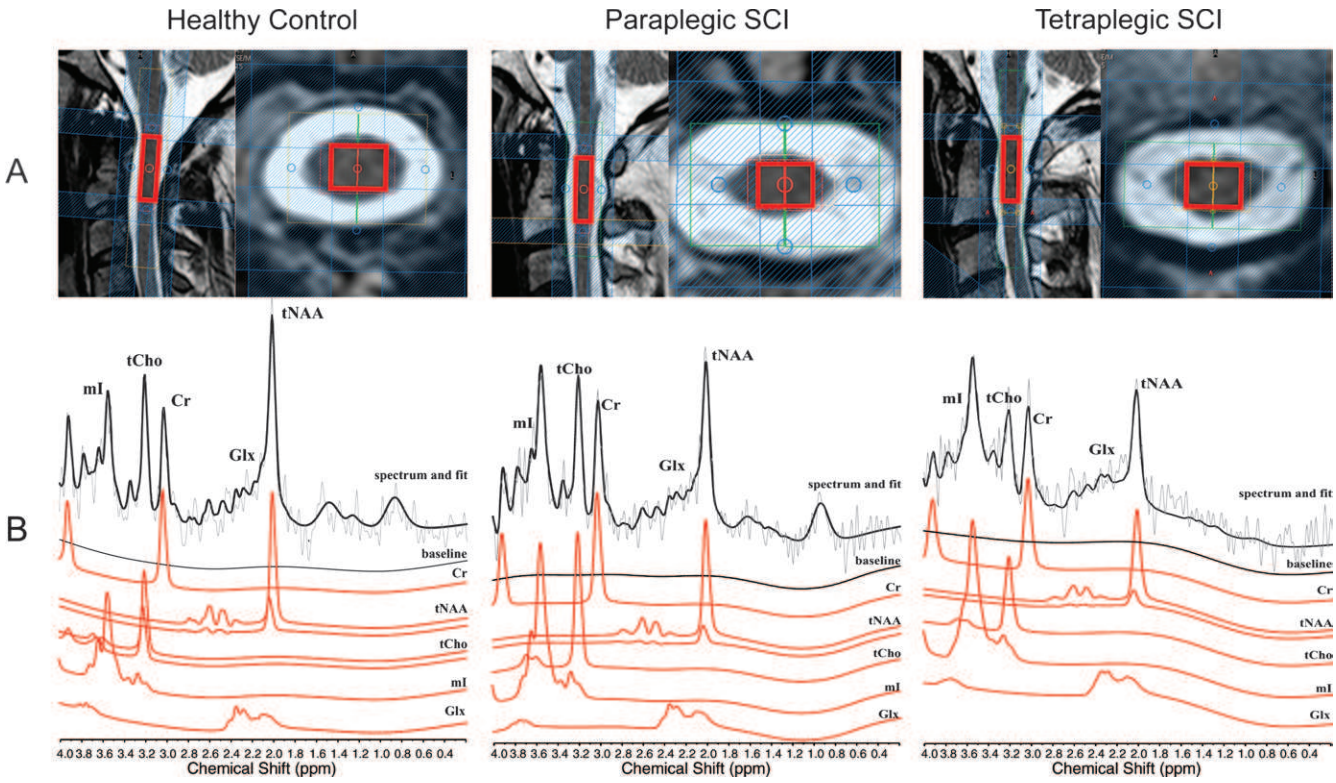

Figure 1: MR spectroscopic voxel localization and representative spectra. *A,* Placement of the spectroscopic voxel of interest. A representative spectrum (background in gray) in a healthy control subject, a participant with paraplegic spinal cord injury *(SCI)*, and a participant with tetraplegic SCI. The resulting fits (black) are shown in *B*. The metabolic components identified in the fit in *B* are given in red for creatine *(Cr)*, total *N*-acetylaspartate *(tNAA)*, total choline-containing compounds *(tCho)*, myo-inositol *(mI)*, and glutamine and glutamate complex (*Glx)*. *ppm* = Parts per million.

at the MR spectroscopy workshop (Lake Constance, August 2016), metabolites were included in case the Cramér-Rao lower bounds were smaller than 100% (15). All MR spectroscopy acquisitions were performed by a trained spectroscopist (P.O.W., with 5 years of experience) without knowledge about the clinical status of the participants. Data analysis was performed by using an automated processing pipeline.

Postprocessing of MRI data above the level of injury.—The cross-sectional spinal cord area (SCA) above the level of injury was assessed (by E.H.) on the T2-weighted images using Jim 6.0 (Xinapse Systems, Aldwincle, England) in all participants as previously described (16). In three participants, manual correction of the surface outline was necessary.

In tetraplegic participants, lesion severity was assessed on the midsagittal section of the T2-weighted images by using Jim 6.0 as previously described (2). At the level of injury, the midsagittal anteroposterior lesion width, the midsagittal rostrocaudal lesion length, the total midsagittal lesion area, and the thickness of the midsagittal ventral and dorsal tissue bridges (total amount of tissue bridges) were quantified (Fig E2 [online]).

Statistical Analysis

For statistical analysis, we used R software, version 3.3.1 (R Team, 2016, Vienna), including ggplot2 (17) for visualization. Boxplots show data including medians and quartiles; medians and ranges are reported in the text.

Kruskal-Wallis tests followed by pairwise Mann-Whitney *U* tests were performed to assess group differences. The Spearman rank correlation test was used to investigate the relationships of the metabolite ratios and atrophy, injury level, and clinical outcome (unadjusted and adjusted for SCA).

The confidence interval was set to 95%, and $P < .05$ was considered to indicate a significant difference. To reduce type II error, we did not adjust for multiple comparisons, which potentially increased the rate of type I errors. Age was included in the statistical model as a covariate of no interest.

Results

Demographics

We included nine participants with a paraplegic injury (injury below neurologic level T1 of the spinal cord) (median age, 48 years; range, 39–54 years), nine participants with a tetraplegic injury (injury above level T2) (median age, 57 years; range, 30–68 years), and 11 healthy control participants (median age, 45 years; range, 30–67 years) in the study. There was no significant difference in age between any of the groups ($P = .22$). All participants were male; the demographic data are summarized in the Table.

All study participants completed the MRI examination and clinical assessment. The mean age at injury and the mean number of years since injury, respectively, were 33 years (range, 14–48 years) and 19 years (range, 2–29 years) for the paraplegic

Clinical and Epidemiologic Data for All Participants with SCI in the Study

Demographic Data			ISNCSCI Findings		Outcome Measures			
Participant No.	Age at Injury (y)	Time Since Injury (y)	AIS Score	Level of Injury	Motor Score	Light Touch Score	Pinprick Score	SCIM Score
1	30	13	D	C2	75	55	55	74
2	51	6	D	C2*	86	56	26	48
3	28	2	A	C4	11	23	23	18
4	31	2	A	C4	22	31	20	28
5	46	12	C	C4	97	112	97	100
6	60	4	D	C4	89	79	64	100
7	41	24	A	C5	38	22	20	63
8	24	31	B	C5	31	68	68	64
9	50	13	D	C7	91	110	107	100
10	44	10	A	T2	50	39	41	58
11	19	27	A	T4	50	71	72	73
12	33	19	A	T4	50	51	48	75
13	14	25	B	T4	50	78	78	66
14	19	29	B	T4	50	50	50	73
15	26	20	A	T5	50	48	48	68
16	46	7	A	T11	67	87	82	69
17	48	2	D	T12	100	94	82	98
18	36	4	D	L1	92	106	104	98

Note.—AIS = American Spinal Injury Association Impairment Scale, ISNCSCI = International Standards for Neurological Classification of Spinal Cord Injury, SCI = spinal cord injury, SCIM = Spinal Cord Independence Measure.

* Small cyst (<10% of the voxel volume) at C2.

participants and 41 years (range, 24–60 years) and 12 years (range, 2–31 years) for the tetraplegic participants. Paraplegic and tetraplegic participants did not significantly differ in terms of age at injury (P = .34) or in the number of years since injury (P = .42). Eight participants with SCI were classified as being in functionally complete condition (American Spinal Injury Association Impairment Scale [AIS] score A), and 10 were classified as being in functionally incomplete condition (AIS score B–D) (Table).

Quality of MR Spectroscopy Measurements

Representative spectra acquired in the spinal cord at level C2 are shown in Figure 1 (the spectroscopic voxel of interest placement is shown in *A*; measured spectra and fitting results with separate metabolite components are shown in *B*) for a healthy control participant, a paraplegic participant, and a tetraplegic participant. No measurement block had to be excluded because of motion. Valid concentration values could be determined for all metabolites in all participants, with the exception of Glx. Glx could not be determined and zero was assumed in one healthy control subject and one paraplegic participant. No differences in metabolite line width (full-width at half-maximum of the NAA peak) between healthy control subjects and participants with SCI was found (P = .51). The volume of interest between measurement blocks was adjusted in two paraplegic participants, in two tetraplegic participants, and in three healthy control participants because of motion. The signal-to-noise ratios of the spectra in the spinal cord were satisfactory; they were a mean of 6 (range, 4–8) in healthy control participants, a mean of 6 (range, 4–7) in participants with paraplegic SCI, and a mean of 5 (range, 4–8) in participants with tetraplegic SCI. Additional quality measures can be found in Table E1 (online).

Metabolic Changes in the Severely Atrophied Cervical Spinal Cord

In participants with SCI, cross-sectional SCA at C2 was 17% smaller than in control participants (P < .001), with more pronounced changes in tetraplegic participants (−25%, P < .001) than in paraplegic participants (−10%, P = .005).

In terms of metabolic changes within this atrophied cord area, we found lower tNAA/mI and tCho/mI ratios in participants with SCI than in control participants (tNAA/mI: −26%, P = .003; tCho/mI: −18%, P = .04) (Fig 2, *A, C*). This group difference was mainly driven by the tetraplegic participant group, which differed from the healthy control group (tNAA/mI: −43%, P = .002; tCho/mI: −25%, P = .03), whereas paraplegic participants only showed a trend toward lower ratios (tNAA/mI: −21%, P = .05; tCho/mI: −17%, P = .22) (Fig 2, *B, D*). Tetraplegic participants had lower tNAA/mI ratios than paraplegic participants (−28%, P = .04), but no difference between subgroups was detected for tCho/mI (−9%, P = .25). Participants with greater cord atrophy had lower levels of tNAA/mI (R^2 = 0.44, P = .003) and showed the same trend for tCho/mI (R^2 = 0.166, P = .09) (Fig 3). No differences were found for mI/Cr (P = .07) (Fig E3, *A, B* [online]).

Relationship between Lesion Characteristics, Metabolic Changes at C2 Level, and Clinical Outcome

Lesion level was positively associated with tNAA/mI (R^2 = 0.402, P = .005) and showed the same trend for tCho/mI (R^2 =

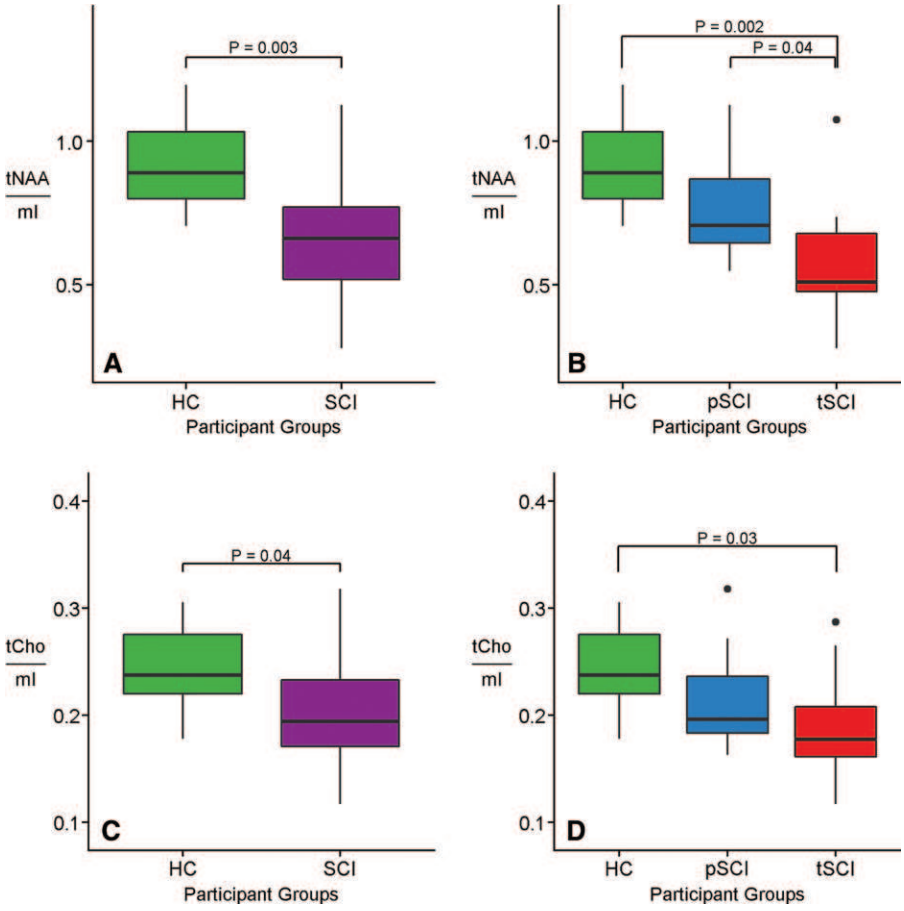

Figure 2: Graphs show group differences in metabolic ratios. The group differences in, *A, B,* the ratios of total *N*-acetylaspartate to myo-inositol (tNAA/mI) and, *C, D,* the ratios of total choline-containing compounds to myo-inositol (tCho/mI) are shown for healthy control participants *(HC)*, participants with spinal cord injury *(SCI)*, and participants with paraplegic SCI *(pSCI)* and tetraplegic SCI *(tSCI)*. Differences are labeled, and uncorrected *P* values are noted.

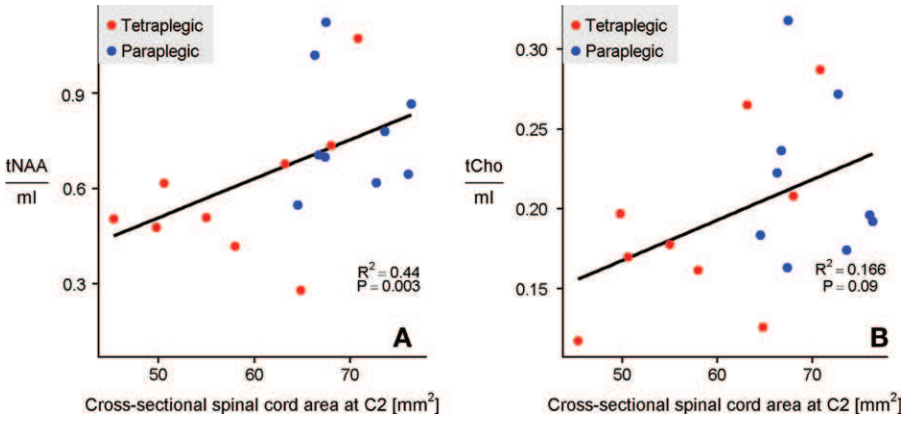

Figure 3: Graphs show spinal cord atrophy and metabolic ratios. The cross-sectional spinal cord area at level C2 is shown in participants with spinal cord injury as rank correlations with, *A,* the ratios of total *N*-acetylaspartate to myo-inositol (tNAA/mI) and, *B,* total choline-containing compounds to myo-inositol (tCho/mI).

0.201, $P = .06$) (Fig 4, *A, B*). When we looked only at participants with complete injury (ie, those with an American Spinal Injury Association Impairment Scale score of A), we found associations between lesion level and both tNAA/mI ($R^2 = 0.613$, $P = .02$) and tCho/mI ($R^2 = 0.711$, $P = .01$) (Fig 4, *C, D*). Furthermore, a higher tNAA/tCho ratio was associated with time since injury ($R^2 = 0.358$, $P = .009$) (Fig 5, *A*) but did not differ between participants with complete injury and those with incomplete injury ($P = .69$) (Fig 5, *B*). In tetraplegic participants, the size of midsagittal tissue bridges at the lesion site was positively correlated with tNAA/mI ($R^2 = 0.686$, $P = .006$) as well as tCho/mI ratios ($R^2 = 0.506$, $P = .03$) above the level of injury (Fig E2, *B, C*). No correlation was found between mI/Cr and clinical scores.

The tNAA/mI and Cho/mI ratios were positively associated with SCIM score (tNAA/mI: $R^2 = 0.560$, $P < .001$; tCho/mI: $R^2 = 0.458$, $P = .002$) and pinprick score (tNAA/mI: $R^2 = 0.353$, $P = .009$; tCho/mI: $R^2 = 0.415$, $P = .004$) (Fig 6, *A–D*). In addition, lower levels of tCho/mI were associated with lower light touch ($R^2 = 0.529$, $P = .001$) and motor ($R^2 = 0.531$, $P = .001$) scores (Fig 6, *E, F*). When adjusted for SCA, tNAA/mI ratio remained associated with SCIM score ($R^2 = 0.606$, $P = .03$), while tCho/mI remained associated with light touch ($R^2 = 0.620$, $P = .03$) and motor ($R^2 = 0.641$, $P = .02$) scores.

Discussion

Demyelination, altered cell and membrane integrity, and activated astrocytes (11) occur remote to the site of traumatic spinal cord injury (SCI). Patients with chronic SCI may therefore exhibit altered metabolism in the atrophied cervical cord above the level of injury. We found that total tNAA/mI and tCho/mI ratios were lower in the atrophic cervical cord in participants with chronic SCI, with more pronounced changes in tetraplegic participants than in paraplegic participants. The more caudal the lesion level, the higher the ratios of tNAA/mI and tCho/mI and the closer the values to those of healthy control subjects. In addition, tNAA/mI and tCho/mI ratios were positively associated with sensory and motor scores, and these associations persisted even when adjusted for SCA. This indicates that pathologic processes are reflected by metabolite concentrations independently of spinal cord atrophy. Therefore, spinal cord spectroscopy above the level of

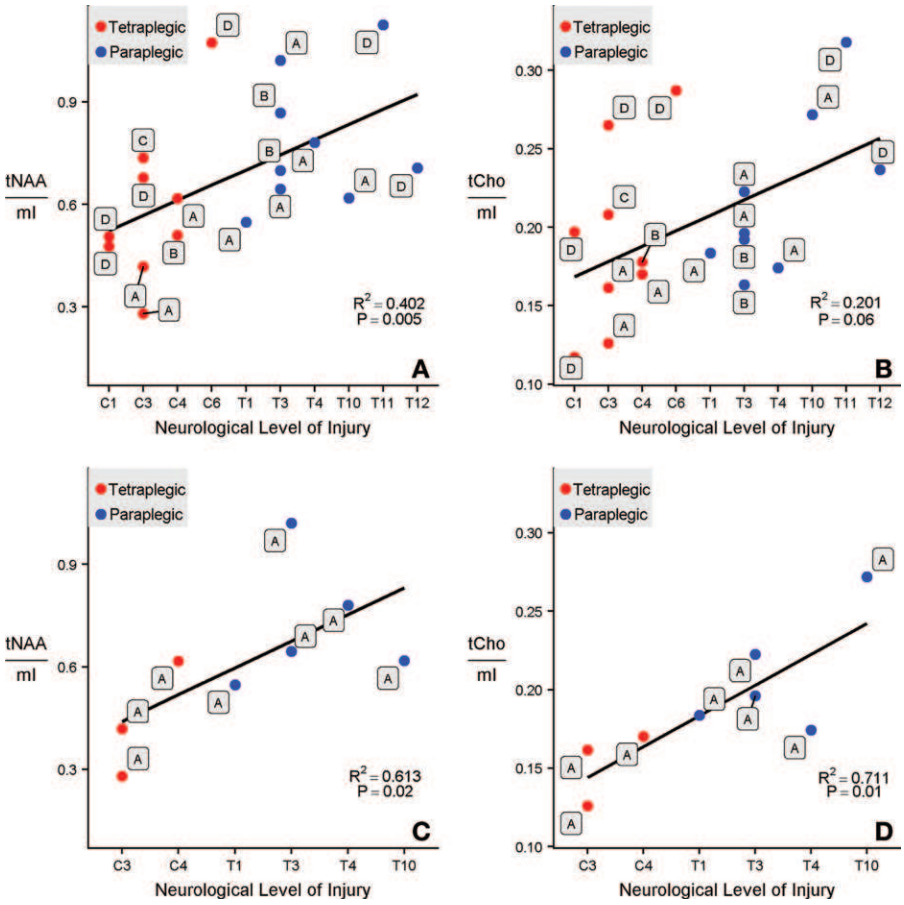

Figure 4: Graphs show lesion proximity and metabolic ratios. The rank correlations of, *A, C,* the neurologic level of injury (C1 to T12) and the ratios of total *N*-acetylaspartate to myo-inositol (tNAA/mI) and, *B, D,* the neurologic level of injury (C1 to T12) and the ratios of total choline-containing compounds to myo-inositol (tCho/mI) are shown. The participants' data are labeled according to their American Spinal Injury Association Impairment Scale (AIS) scores from A to D. All participants with spinal cord injury are included in *A* and *B*, whereas only participants with complete injury (ie, AIS score A) are included in *C* and *D*.

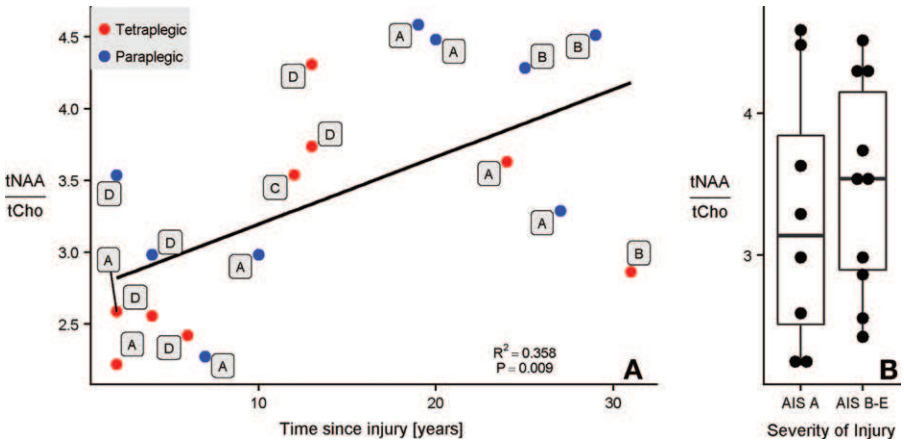

Figure 5: Graphs show lesion characteristics and metabolic ratios. *A,* Rank correlation between the time since injury (in years) and the ratio of total *N*-acetylaspartate to total choline-containing compounds *(tNAA/tCho). B,* The ratio of tNAA/tCho is shown for participants with complete injury (American Spinal Injury Association Impairment Scale *[AIS]* score A) versus participants with incomplete injury (AIS scores B, C, D, and E).

injury may help improve outcome prediction and, potentially, monitor treatment effects in clinical trials.

The observed reductions in tNAA/mI and tCho/mI ratios can be attributed to either lower levels of NAA and choline and/or higher levels of mI. NAA is synthesized in the mitochondria of neurons from aspartic acid and acetyl coenzyme A (18) and is predominantly present in neuronal cell bodies and axons. This suggests that decreased NAA reflects a combination of axonal/neuronal loss (19) and reduced mitochondrial metabolism (20). It has been further suggested that acetate (from degradation of NAA) is used to build lipids for maintaining myelination (21). Thus, a reduction in NAA might also relate to demyelination. In line with this, higher mI levels likely indicate the presence of activated astrocytes, which produce chondroitin sulfate proteoglycans as well as keratins, which inhibit axonal regeneration (22). On the other hand, total choline receives contribution from free choline, glycerophosphocholine, and phosphocholine, which are precursors of cell membrane synthesis (23) and of the neurotransmitter acetylcholine (23). Total choline is typically increased when there is increased membrane turnover or when there is inflammation (24). In multiple sclerosis, choline is typically increased in acute phases of demyelination as the degradation of myelin leads to the release of phosphatidylcholine (25).

Animal studies investigating the choline concentration after SCI (26) reported highly elevated levels of choline early after injury. These results suggest that after SCI, there is an initial high membrane turnover because of cell membrane breakdown and/or demyelination that levels off over time, as there are fewer viable neurons capable of undergoing membrane turnover.

Next to the observed metabolic changes within areas of cord atrophy, the tNAA/mI ratio was positively associated with the severity of cord atrophy. This indicates that not only do patients with a smaller SCA

have more pronounced neurodegeneration but also that the structure within the cord is altered. Postmortem studies of humans with SCI suggest that damaged spinal neurons may be partly replaced by fibrous connective tissue and collagen (27), which might account for this finding. In addition, we showed that lesion level was positively associated with tNAA/mI. Thus, the larger the initial damage at the lesion site, the more axons above the level of injury may undergo retro- and anterograde degeneration. This progressive degeneration and change in molecular content are of particular importance when treatments are investigated, as treatments in patients with SCI should ideally start as early as possible to prevent further structural damage.

Interestingly, these ratio changes are comparable to cervical changes observed in other neurodegenerative diseases like multiple sclerosis (5), amyotrophic lateral sclerosis (6), and Friedreich ataxia (7). For example, Carew et al (6) observed 38% lower tNAA/mI ratios in patients with amyotrophic lateral sclerosis and smaller tCho/mI ratios compared with those in control subjects. This is comparable to what we observed (−26% for tNAA/mI and −18% for tCho/mI). Our study complements these studies by showing for the first time (to our knowledge) that cervical metabolic changes also occur in participants with SCI. In contrast to other studies, we also examined the relationship between lesion level and metabolic alterations.

Our study had important limitations. Metabolic values are presented as ratios to other metabolites and not as absolute values. Although absolute quantification is possible in the brain by means of referencing the internal water signal, this is not yet possible in the spinal cord because the water reference scan in the spinal cord is affected by the surrounding cerebrospinal fluid owing to the partial-volume effect and thus does not serve as a reliable and valid reference. In addition, our study participant number in each group was small. We therefore only included men to homogenize our groups, but future studies will also include female participants. Furthermore, the long protocol examination time was a major impediment and still hampers a rapid translation of spinal cord MR spectroscopy to clinical diagnostics. However, at this stage, proton MR spectroscopy can be used for clinical studies with respect to therapy response.

In conclusion, we showed that metabolite ratios estimated from short-echo MR spectroscopy correlate more strongly with the clinical status of the patient than with volumetric measures of the spinal cord alone. This may improve outcome prediction and patient stratification and prove valuable in future clinical trials related to different therapy options.

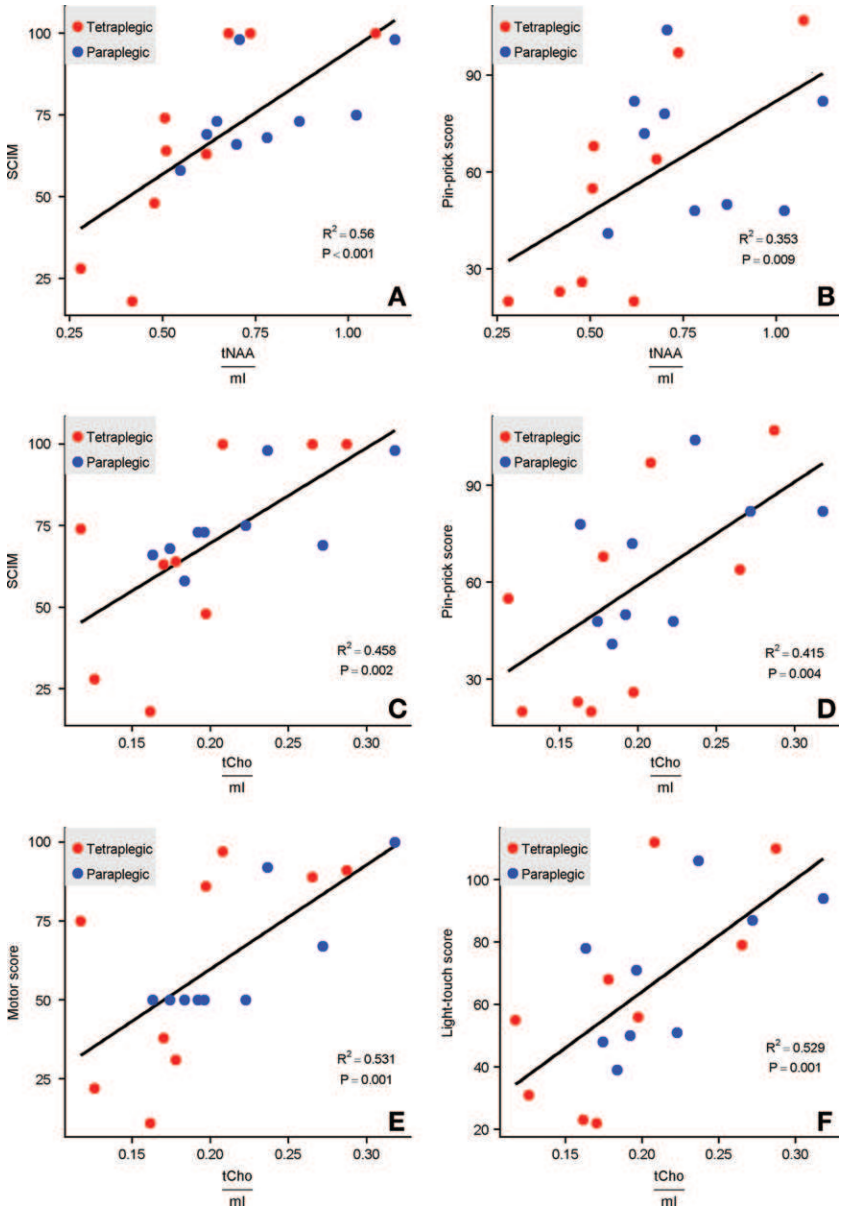

Figure 6: Graphs show metabolic ratios and outcome measures. *A, B,* Graphs show the correlations of the metabolic ratios of total *N*-acetylaspartate to myo-inositol (tNAA/mI) and, *C–F,* total choline-containing compounds to myo-inositol (tCho/mI) in participants with spinal cord injury with outcome measures, including Spinal Cord Independence Measure *(SCIM)* (in *A, C*), pinprick score (in *B, D*), motor score (in *E*), and light touch score (in *F*).

Acknowledgments: The authors are grateful to the patients and healthy volunteers who participated in this study. Special thanks go to Céline Steger, BSc, and Desiree Beck, MSc, for their help in recruiting and assessing the participants.

Author contributions: Guarantors of integrity of entire study, P.O.W., E.H., A.H.; study concepts/study design or data acquisition or data analysis/interpretation, all authors; manuscript drafting or manuscript revision for important intellectual content, all authors; manuscript final version approval, all authors; agrees to ensure any questions related to the work are appropriately resolved, all authors; literature research, P.O.W., E.H., P.F., A.H.; clinical studies, E.H., P.F.; experimental studies, P.O.W., E.H., A.H.; statistical analysis, P.O.W., E.H., P.F.; and manuscript editing, P.O.W., E.H., P.F., A.H.

Disclosures of Conflicts of Interest: **P.O.W.** disclosed no relevant relationships. **E.H.** disclosed no relevant relationships. **A.C.** disclosed no relevant relationships. **S.K.** disclosed no relevant relationships. **P.F.** disclosed no relevant relationships. **A.H.** disclosed no relevant relationships.

References

1. Freund P, Weiskopf N, Ward NS, et al. Disability, atrophy and cortical reorganization following spinal cord injury. Brain 2011;134(Pt 6):1610–1622.
2. Huber E, Lachappelle P, Sutter R, Curt A, Freund P. Are midsagittal tissue bridges predictive of outcome after cervical spinal cord injury? Ann Neurol 2017;81(5):740–748.
3. Huber E, Curt A, Freund P. Tracking trauma-induced structural and functional changes above the level of spinal cord injury. Curr Opin Neurol 2015;28(4):365–372.
4. Hock A, MacMillan EL, Fuchs A, et al. Non-water-suppressed proton MR spectroscopy improves spectral quality in the human spinal cord. Magn Reson Med 2013;69(5):1253–1260.
5. Abdel-Aziz K, Schneider T, Solanky BS, et al. Evidence for early neurodegeneration in the cervical cord of patients with primary progressive multiple sclerosis. Brain 2015;138(Pt 6):1568–1582.
6. Carew JD, Nair G, Pineda-Alonso N, Usher S, Hu X, Benatar M. Magnetic resonance spectroscopy of the cervical cord in amyotrophic lateral sclerosis. Amyotroph Lateral Scler 2011;12(3):185–191.
7. Lenglet C, Joers J, Pisharady P, et al. Cross-sectional and longitudinal diffusion MRI and MRS of the spinal cord in Friedreich's Ataxia. In: Proc of the Hum Brain Mapp, 2016; 1245.
8. Hock A, Petrou N, Zweers P, et al. MR spectroscopy in the spinal cord of patients with traumatic injuries [abstr]. In: Proceedings of the Twentieth Meeting of the International Society for Magnetic Resonance in Medicine. Berkeley, Calif: International Society for Magnetic Resonance in Medicine, 2012; 1047.
9. Wyss PO, Huber E, Freund P, Henning A. Spinal cord MRS biomarkers of clinical impairment in chronic spinal cord injury [abstr]. In: Proceedings of the Twenty-Sixth Meeting of the International Society for Magnetic Resonance in Medicine. Berkeley, Calif: International Society for Magnetic Resonance in Medicine, 2018; 670.
10. Wyss PO, Huber E, Freund P, et al. Cervical spinal cord proton spectroscopy and impairment in spinal cord injury at 3T. In: Proc of the Hum Brain Mapp, 2017; 3578.
11. Rust R, Kaiser J. Insights into the dual role of inflammation after spinal cord injury. J Neurosci 2017;37(18):4658–4660.
12. Kirshblum SC, Burns SP, Biering-Sorensen F, et al. International standards for neurological classification of spinal cord injury (revised 2011). J Spinal Cord Med 2011;34(6):535–546.
13. Itzkovich M, Gelernter I, Biering-Sorensen F, et al. The Spinal Cord Independence Measure (SCIM) version III: reliability and validity in a multi-center international study. Disabil Rehabil 2007;29(24):1926–1933.
14. Provencher SW. Estimation of metabolite concentrations from localized in vivo proton NMR spectra. Magn Reson Med 1993;30(6):672–679.
15. Kreis R. The trouble with quality filtering based on relative Cramér-Rao lower bounds. Magn Reson Med 2016;75(1):15–18.
16. Horsfield MA, Sala S, Neema M, et al. Rapid semi-automatic segmentation of the spinal cord from magnetic resonance images: application in multiple sclerosis. Neuroimage 2010;50(2):446–455.
17. Wickham H. ggplot2: Elegant Graphics for Data Analysis. New York, NY: Springer-Verlag, 2009.
18. Truckenmiller ME, Namboodiri MA, Brownstein MJ, Neale JH. N-acetylation of L-aspartate in the nervous system: differential distribution of a specific enzyme. J Neurochem 1985;45(5):1658–1662.
19. Bjartmar C, Kidd G, Mörk S, Rudick R, Trapp BD. Neurological disability correlates with spinal cord axonal loss and reduced N-acetyl aspartate in chronic multiple sclerosis patients. Ann Neurol 2000;48(6):893–901.
20. Bates TE, Strangward M, Keelan J, Davey GP, Munro PM, Clark JB. Inhibition of N-acetylaspartate production: implications for 1H MRS studies in vivo. Neuroreport 1996;7(8):1397–1400.
21. Chakraborty G, Mekala P, Yahya D, Wu G, Ledeen RW. Intraneuronal N-acetylaspartate supplies acetyl groups for myelin lipid synthesis: evidence for myelin-associated aspartoacylase. J Neurochem 2001;78(4):736–745.
22. Silver J, Miller JH. Regeneration beyond the glial scar. Nat Rev Neurosci 2004;5(2):146–156.
23. Wang XC, Du XX, Tian Q, Wang JZ. Correlation between choline signal intensity and acetylcholine level in different brain regions of rat. Neurochem Res 2008;33(5):814–819.
24. Howe FA, Opstad KS. 1H MR spectroscopy of brain tumours and masses. NMR Biomed 2003;16(3):123–131.
25. Richards TL. Proton MR spectroscopy in multiple sclerosis: value in establishing diagnosis, monitoring progression, and evaluating therapy. AJR Am J Roentgenol 1991;157(5):1073–1078.
26. Qian J, Herrera JJ, Narayana PA. Neuronal and axonal degeneration in experimental spinal cord injury: in vivo proton magnetic resonance spectroscopy and histology. J Neurotrauma 2010;27(3):599–610.
27. Norenberg MD, Smith J, Marcillo A. The pathology of human spinal cord injury: defining the problems. J Neurotrauma 2004;21(4):429–440.